Supporting Information

Gupta et al. 10.1073/pnas.1000248107

SI Methods

Cell Culture. GIST-T1, a human cell line established from an untreated GIST with a primary imatinib-sensitive mutation in *KIT* exon 11, was cultured as described (1). GIST-T1-R was derived from GIST-T1 as an imatinib-resistant clone that arose by continuous culture in 5 μM imatinib. In addition to the original 57-base pair *KIT* exon 11 deletion, there is a missense mutation encoding KIT T670I, a mutation frequently found in GIST that has developed secondary resistance to imatinib (2). GIST-T1-R cells were cultured as described for GIST-T1. GIST882 is a human cell line established from an untreated GIST with a primary imatinib-sensitive mutation in *KIT* exon 13, and cultured as described (3, 4).

Antibodies and Chemicals. A described α-LC3 rabbit polyclonal sera was used for immunoblotting (5). Commercial antibodies that were used include p27, LAMP2, ATG7 (Santa Cruz Biotechnology); S6, phospho-S6 (Ser235/236), eIF2α, phospho-eIF2α (Ser51), ATG12, (Cell Signaling); p62 (Progen), β-actin, and α-tubulin (Sigma-Aldrich). Chemicals used included imatinib mesylate (LC Laboratories) and quinacrine, bafilomycin A1, chloroquine, E64d, and pepstatin A (Sigma-Aldrich).

Generation of Stable Lines. pBABEpuro-GFP-LC3 has been described and was used to stably express this fusion in GIST-T1 cells (5). pBABEpuro-mCherry-GFP-LC3 (6) was used to stably express this fusion protein in GIST-T1 cells.

Cell-Cycle Analysis. Cells were trypsinized, centrifuged, washed once with PBS solution, fixed in ice cold ethanol, and stored at −20 °C. After washing with PBS, cells were treated with PBS containing RNase A at 1 mg/mL, and propidium iodide (Sigma-Aldrich) at 50 μg/mL DNA content was analyzed on a fluorescence-activated cell analyzer (FACScan; Becton Dickinson). Cell cycle profiles were determined by using MODFIT LT3.0 (Verity Software).

Cell Proliferation and Apoptosis Analyses. Three thousand cells per well were plated in complete media in 96-well flat-bottom plates. After 24 h, cells were incubated as indicated. Proliferation was evaluated by the Trypan blue exclusion method. Cells were plated in triplicate, and each experiment was performed three times. Apoptosis was evaluated by measuring caspase-3/7 activity by Caspase Glo-3/7 assay system (Promega); luminescence was measured by using a Wallac 1420 multilabel counter (Perkin-Elmer). Caspase inhibitor Z-VAD-fmk (Biomol) was used at 20 μM concentration wherever indicated as a control. For TUNEL assay, 20,000 cells were seeded in four chamber slides, treated with 1 μM imatinib for 48 h, and stained with TUNEL assay kit per manufacturer's instructions (Promega).

Glucose Uptake Analysis. Cells were treated with imatinib for 24 h and then incubated with 100 μM 2-[*N*-(7-nitrobenz-2-oxa-1,3-diazol-4-yl)amino]-2-deoxy-glucose (2-NBDG; Invitrogen) for 15 min, cells were washed with PBS, and detached with 0.05% trypsin. The relative fluorescence intensity of cells was measured by using a fluorescence-activated cell analyzer (FACScan; Becton Dickinson) and analyzed by using FlowJo v6.4.1 software (TreeStar).

Analysis of Punctate GFP-LC3 and GFP-mCherry-LC3. Cells stably expressing either GFP-LC3 or GFP-mCherry-LC3 were grown overnight before treatment with imatinib for the indicated times. Cells were fixed with 4% paraformaldehyde, washed several times with PBS, mounted by using Vectashield with 4′-6-diamidino-2-phenylindole (DAPI) (Vector Laboratories), and analyzed at 20 °C by widefield immunofluorescent microscopy using the ×63 [1.4 numerical aperture (NA)] or 100× (1.3 NA) objectives of an Axiovert 200 microscope (Carl Zeiss) equipped with a Spot RT camera (Diagnostic Instruments) and mercury lamp. Images were acquired by using MetaMorph (version 6.0) software (GE Healthcare). Confocal analysis of GFP-mCherry LC3 expressing cells was performed at 20 °C by using the 60× (1.4 NA) objective of a Nikon C1si Spectral Confocal System (located in the UCSF Biological Imaging Development Center) equipped with an argon laser (488 line) and solid state diode (546 line). Quantification of punctate LC3 was performed using Metamorph (v6.0).

Immunohistochemistry. Formalin-fixed paraffin embedded tissue sections were cut at 4 μM for use in immunohistochemistry on a Discover XT automated stainer (Ventana Medical Systems).
LC3. Antigen retrieval consisted of CC1 (Tris/Borate/EDTA buffer, pH 8.0–8.5) (Ventana) for 44 min at 95 °C. Tissue sections were then incubated with primary α-LC3 antibody (mouse monoclonal, clone 5F10; NanoTools/Axorra) for 1 h at room temperature. Secondary antibody (OmniMap anti-Ms HRP; Ventana) was applied for 12 min, and ChromoMap DAB (Ventana) was used for detection. Cells were counterstained with hematoxylin and visualized by light microscopy.
Cleaved caspase-3. Antigen retrieval consisted of RiboCC (Citrate buffer, pH 6.0; Ventana) for 8 min at 95 °C, 12 min at 100 °C, and then an 8-min cool down to 37 °C. Primary Cleaved Caspase-3 (Asp-175) antibody (rabbit polyclonal; Cell Signaling) was incubated for 44 min at room temperature. Secondary antibody (OmniMap anti-Rb HRP; Ventana) was applied for 16 min and ChromoMap DAB (Ventana) was used for detection. Cells were counterstained with hematoxylin and visualized by light microscopy. Cleaved caspase-3–positive cells were enumerated in five high-power (400×) fields.

Clonogenic Replating Assay. Cells were grown under various conditions, treated with 0.05% trypsin-EDTA at 37 °C for 5 min to generate single cell suspensions, and cells were counted and replated in complete growth media at 100 cells per well onto six-well tissue culture plates. Colonies were grown out for 7–14 d, fixed with methanol, and stained with 0.2% crystal violet. The number of colonies was enumerated, and replating efficiency was calculated as the number of colonies growing out divided by the original number of cells plated. For each experiment, six replicates were performed for each condition tested, and each experiment was repeated three times.

RNA Interference. Pooled small interfering RNA (siRNA) oligonucleotides (ON-TARGET plus SMARTpool) against *ATG7*, *ATG12*, or *LAMP2* were purchased from Dharmacon RNAi Technologies. For siRNA transfection, cells were seeded at 100,000 per well in 100-mm tissue culture dishes, and they were transfected with 50–100 nM of the pooled oligonucleotide mixture by using Oligofectamine (Invitrogen) following manufacturer's protocols. The transfection media were removed, and cells were allowed to recover in complete growth media for 36–48 h before use in experiments. The sense sequences of the individual duplexes directed against *ATG7*, *ATG12*, and *LAMP2* are as follows: *ATG7* (NM_006395): CCAACACACUCGAGUCUUU, GAUCUAAAUCUCAAACUGA, GCCCACAGAUGGAGUAGCA, and GCCAGAGGAUUCAACAUGA. *ATG12* (NM_004707): GAACACCAAGUUUCACUGU, GCAGUAGAGCGAACACGAA, GG-

GAAGGACUUACGGAUGU, and GGGAUGAACCACAAAGAAA. *LAMP2* (NM_002294): CUCAAUAGCAGCACCAUUA, GCAUGUAUUUGGUUAAUGG, GCAUUGGAACUUAAUUUGA, and AAAUGCCACUUGCCUUUAU.

Immunoblot Analysis. Cells were lysed in radioimmunoprecipitation assay buffer (1% Triton X-100, 1% sodium deoxycholate, 0.1% SDS, 25 mM Tris at pH 7.6, 150 mM NaCl, 10 mM NaF, 10 mM β-glycerophosphate, 1 mM Na_3VO_3, and 10 nM calyculin A plus protease inhibitors). Lysates were cleared by centrifugation for 15 min at 4 °C, boiled in SDS sample buffer, resolved by using SDS/PAGE, and transferred to polyvinylidene difluoride membrane. The membranes were blocked in PBS + 0.1% Tween-20 with 5% nonfat dry milk, incubated with the primary antibodies indicated overnight at 4 °C, washed, incubated with horseradish peroxidase-conjugated secondary antibodies, and analyzed by enhanced chemiluminescence.

Electron Microscopy. Specimens were fixed in 3.75% glutaraldehyde, 0.1 M sodium cacodylate, 6% sucrose at pH 7.2–7.4 for a period of 4 h to overnight. Specimens were postfixed in 1% osmium tetroxide, 0.1 M cacodylate at pH 7.2–7.4 for 1 h. After each fixation step, specimens were washed twice in cacodylate buffered sucrose, 10 min each. After the final wash, specimens were dehydrated in ascending graded alcohols, followed by immersion in propylene oxide, then passed through ascending graded mixtures of EMBed 812 epoxy resin and propylene oxide, and finally embedded in pure epoxy resin. Specimen blocks were polymerized overnight at 60 °C. Specimens were initially evaluated by light microscopy of 1-μm plastic sections stained in a combination of toluidine blue and basic fuchsin. Thin sections from selected tissue blocks were cut at 60–80 nm and supported on 200 mesh copper grids. Sections were stained in uranyl acetate and lead citrate, and examined using a Philips CM-12 electron microscope.

Treatment of GIST-T1 Xenografts. Female adult athymic nude mice (NMRI *Nu/Nu*), with an average body weight of 35.8 grams were used to generate heterotopic GIST xenografts. The animals were housed in sterile cages under laminar flow hoods in a temperature controlled room with a 12-h light/12-h dark schedule and fed autoclaved chow and water ad libitum. The animal studies were approved by the Animal Ethics committee of the Catholic University Leuven, Belgium. For inoculation into nude mice, GIST-T1 cells were washed in PBS, digested with trypsin, resuspended in DMEM containing FBS, and pooled. After centrifugation, the cells were resuspended in PBS at a density of 3×10^6 viable cells per 100 μL. The cell suspension (200 μL), was injected s.c. in the right and left flanks of 36 athymic *Nu/Nu* mice. Tumor growth was assessed every other day. Three orthogonal diameters were measured with a Vernier caliper and used to calculate tumor volume. When the tumors reached a volume of ≈500 mm^3, the mice were randomized into 6 groups (12 tumors per group = 6 mice). The first control group received only sterile water. The second group received 50 mg/kg imatinib twice daily by oral gavage. The third group received 60 mg/kg chloroquine daily by i.p. injection. The fourth group received 50 mg/kg quinacrine daily by oral gavage. The fifth group received a combination of chloroquine and imatinib at the dosages stipulated for groups 2 and 3. For the chloroquine and imatinib combination group, mice were pretreated with chloroquine (60 mg/kg per day) for 2 d before treatment with imatinib and chloroquine was initiated. The sixth group received imatinib and quinacrine at the dosages stipulated for groups 2 and 4. Mice were treated for a total of 15 d. When treatment ended, pieces of tumor were either fixed in 10% buffered formalin, or snap frozen in liquid nitrogen.

Human Subjects. The collection and analysis of human tissue samples was approved by the M.D. Anderson Cancer Center Institutional Review Board. Informed consent was obtained from all subjects.

Statistics. All numerical data including error bars represent the mean ± SD. Experimental groups were compared by paired Student's *t* test using GraphPad software when appropriate. To assess for synergy between imatinib and inhibition of autophagy, a repeated measure analysis of variance model, with experiment as the grouping variable was fit. If the interaction was statistically significant, differences between imatinib and combination therapies were evaluated. Synergy analyses were performed by using SAS (version 9.1.3) All tests assumed a 0.05 significance level.

Chou-Talalay Analysis. For the experiment described in Figs. S7 and S8, synergistic, additive, or antagonistic effects of the drug combinations on caspase activity were analyzed by the combination index method of Chou and Talalay (7, 8). CalcuSyn software (version 2.0; Biosoft) is based on this method and takes into account both potency [median dose (Dm)] and the shape of the dose–effect curve (the *m* value) and was used to calculate the combination index (CI). Synergy, additivity, and antagonism are defined as CI < 1, CI = 1, and CI > 1, respectively. For this analysis, imatinib and either chloroquine or quinacrine were combined at fixed ratios of imatinib (0.05, 0.1, 0.5, 1, and 5 μM) with either quinacrine (1, 3, 5, 7, 7.5, or 10 μM) or chloroquine (12.5, 25, 50, 100, and 200 μM). The fraction affected (FA) and the corresponding CI values were calculated for each concentration. Finally, the median effect method was used in the sequential combination studies to identify the most promising schedule of combinations. Triplicate data points were used for each concentration; each experiment was repeated at least twice (n = 6 replicates).

1. Taguchi T, et al. (2002) Conventional and molecular cytogenetic characterization of a new human cell line, GIST-T1, established from gastrointestinal stromal tumor. *Lab Invest* 82:663–665.
2. Heinrich MC, et al. (2006) Molecular correlates of imatinib resistance in gastrointestinal stromal tumors. *J Clin Oncol* 24:4764–4774.
3. Duensing A, et al. (2004) Mechanisms of oncogenic KIT signal transduction in primary gastrointestinal stromal tumors (GISTs). *Oncogene* 23:3999–4006.
4. Lux ML, et al. (2000) KIT extracellular and kinase domain mutations in gastrointestinal stromal tumors. *Am J Pathol* 156:791–795.
5. Fung C, Lock R, Gao S, Salas E, Debnath J (2008) Induction of autophagy during extracellular matrix detachment promotes cell survival. *Mol Biol Cell* 19:797–806.
6. Debnath J (2009) Detachment-induced autophagy in three-dimensional epithelial cell cultures. *Methods Enzymol* 452:423–439.
7. Chou T (1991) The median-effect principle and the combination index for quantitation of synergism and antagonism. *Synergism and antagonism in chemotherapy,* eds Chou TR, Rideout DC (Academic, San Diego), pp 61–102.
8. Chou TC, Talalay P (1984) Quantitative analysis of dose-effect relationships: the combined effects of multiple drugs or enzyme inhibitors. *Adv Enzyme Regul* 22:27–55.

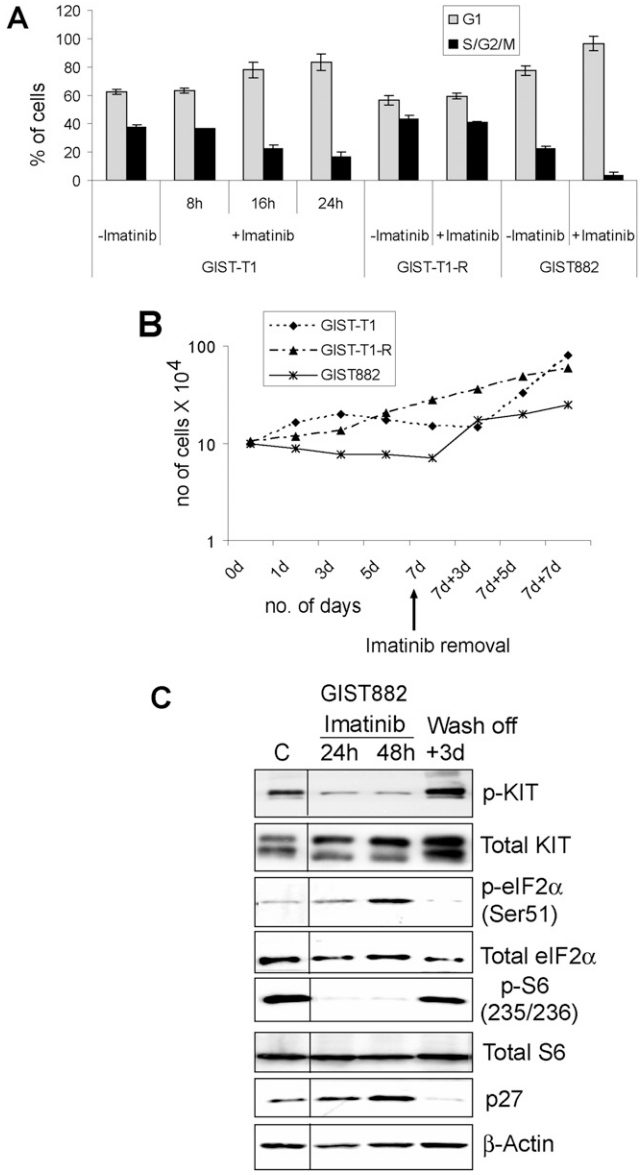

Fig. S1. KIT activation, translational, and cell-cycle arrest induced by imatinib is reversible. (*A*) Cell-cycle analysis by flow cytometry of different GIST cell lines treated with or without 1 μM imatinib for the indicated times. (*B*) Cell counts were determined after treatment with imatinib for the indicated times. Imatinib was removed from the media after 7 d, and cell counts were measured 3, 5, and 7 d after removal. (*C*) Lysates from GIST882 grown in the absence or presence of 1 μM imatinib for the indicated times were immunoblotted with antibodies to KIT, pKIT (Y721), pEIF2α (Ser51), eIF2α, pS6 (Ser235/236), S6, p27, and β-actin.

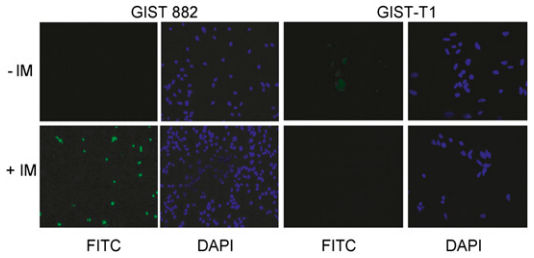

Fig. S2. Variable amounts of apoptosis in different GIST cell lines treated with imatinib. Representative images of the indicated cells grown for 48 h with (*Upper*) or without (*Lower*) 1 μM imatinib, stained for fluorescein-12-dUTP-incorporation by TdT (FITC, green) and counterstained with DAPI (blue) to detect nuclei.

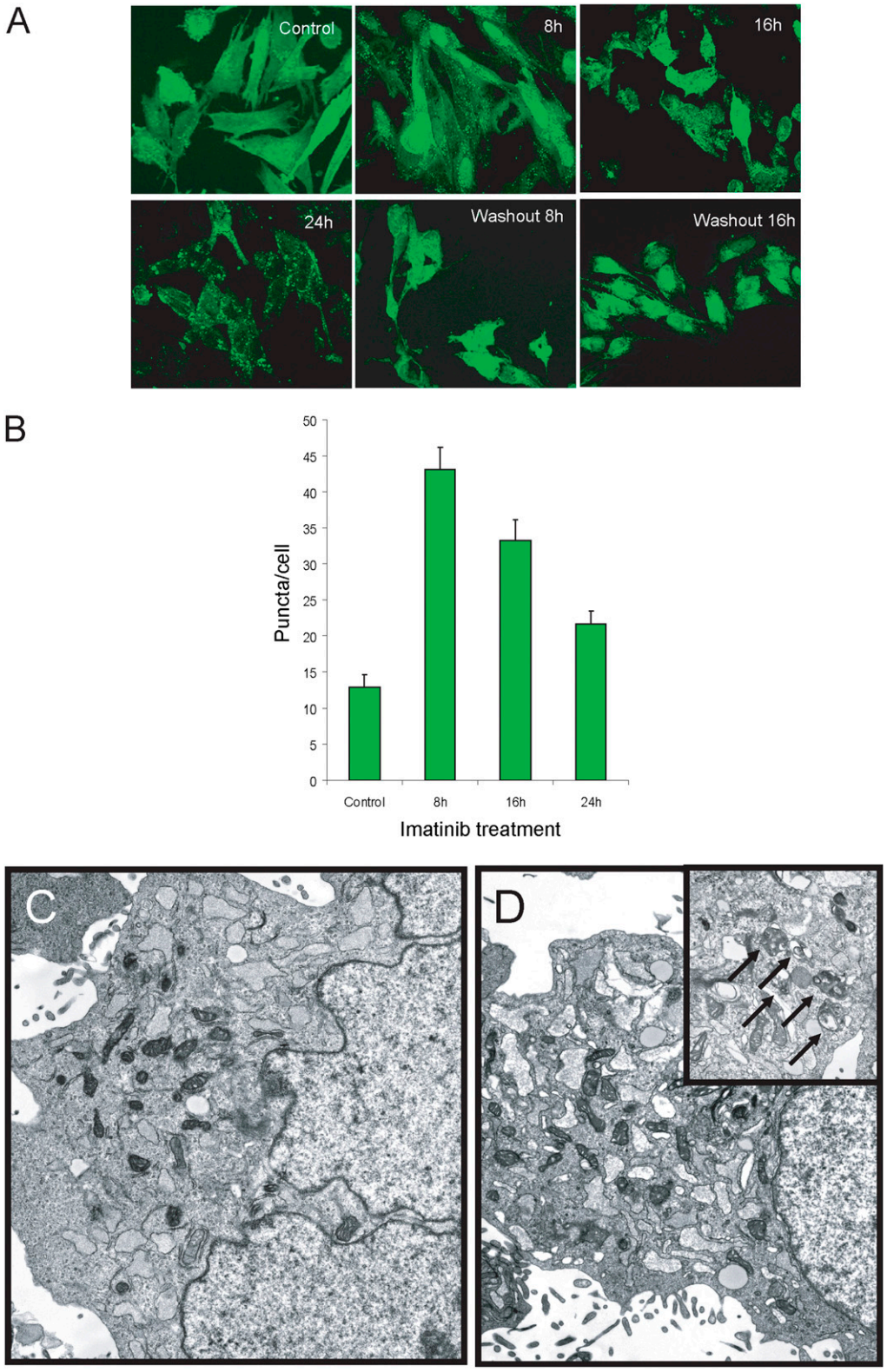

Fig. S3. Imatinib induces autophagosome formation in GIST-T1 cells. (*A*) GFP puncta in GIST-T1 cells expressing GFP-LC3 grown in complete media with 1 μM imatinib for the indicated times. (*B*) Quantification of GFP puncta per cell in control and 1 μM imatinib for the indicated times. (*C* and *D*) Transmission electron micrographs of GIST-T1 cells grown in the absence (*C*) or presence (*D*) of 1 μM imatinib for 8 h. (*Inset*) Arrows indicate autophagic vesicles.

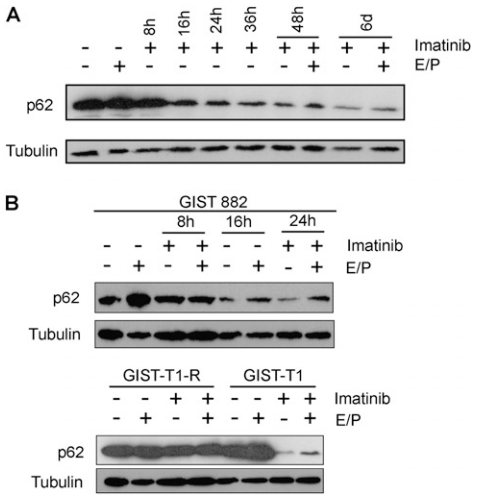

Fig. S4. Imatinib induced degradation of the autophagy substrate p62 (SQSTM) in sensitive GIST cells. (*A*) GIST-T1 cells were treated with 1 μM imatinib for the indicated times, lysed, and subject to immunoblotting for p62 (SQSTM1) or tubulin. (*B*) GIST882, GIST-T1-R, or GIST-T1 cells were treated with 1 μM imatinib for the indicated times, lysed, and immunoblotted with antibodies against p62 or tubulin. When indicated by E/P+, E64d and pepstatin A (10 μg/mL each) were added directly to culture 2 h before lysis.

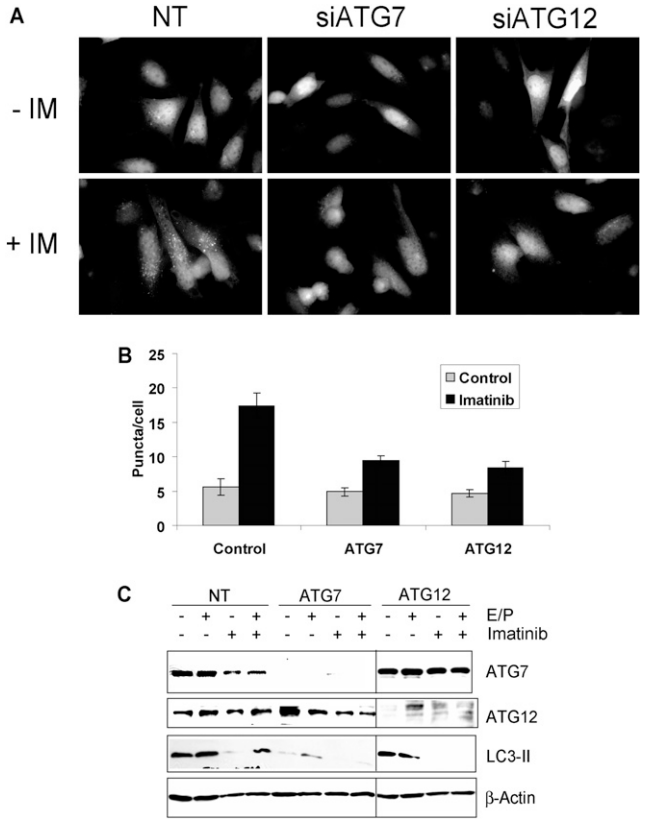

Fig. S5. RNAi-mediated depletion of ATG7 and -12 in GIST-T1 cells. (*A*) GFP puncta in GIST-T1 cells expressing GFP-LC3 grown in complete media with or without 1 μM imatinib after transfection with siRNA pools targeting *ATG7* or *ATG12*. (*B*) Quantification of GFP-positive puncta per cells in control or cells treated with 1 μM imatinib for 24 h. (*C*) Depletion was verified by examining lysates and immunoblotting with antibodies against ATG7, ATG12, or β-actin as indicated. Autophagy was detected in cell lysates by immunoblotting for LC3-II.

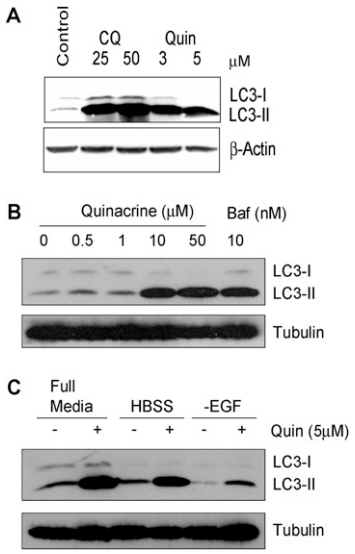

Fig. S6. Quinacrine induces autophagy in GIST-T1 and human epithelial cells. (*A*) Autophagy was evaluated in cell lysates by immunoblotting with antibodies to α-LC3 or β-actin from GIST-T1 after treatment with chloroquine (CQ) or quinacrine (Quin) at the specified doses (micromolars) for 24 h. (*B*) MCF-10A breast epithelial cells were cultured in full media (nutrient and growth factor replete) for 2 h in the presence of quinacrine at the designated concentrations, or in the presence of 10 nM bafilomycin A1 (Baf), a known inhibitor of autophagosome maturation, as a positive control. Lysates were immunoblotted with antibodies to α-LC3 or Tubulin. (*C*) MCF-10A breast epithelial cells were cultured in full media or subject to autophagy induction via HBSS starvation for 6 h or EGF withdrawal for 15 h; when designated, 5 μM Quin was added 2 h before lysis. Lysates were subject to immunoblotting with antibodies to LC3 or Tubulin.

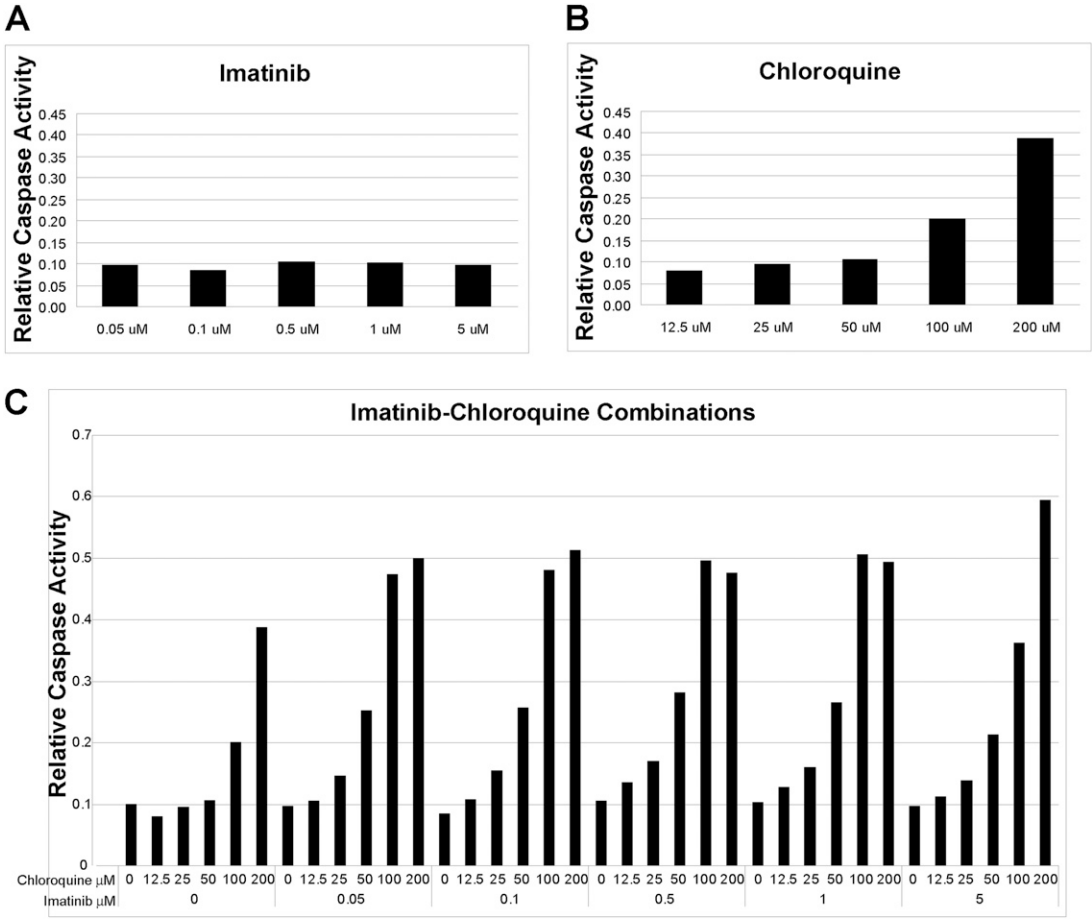

D

Combination Index					
Chloroquine (μM)	Imatinib (μM)				
	0.05	0.1	0.5	1	5
12.5	0.445	0.431	0.296	0.326	0.410
25	0.527	0.478	0.405	0.446	0.568
50	0.394	0.382	0.320	0.360	0.541
100	0.194	0.187	0.171	0.161	0.375
200	0.334	0.311	0.384	0.346	0.194

Fig. S7. Evaluation of synergistic effect on apoptosis between imatinib and chloroquine by Chou–Talalay analysis. Caspase 3/7 activity of GIST-T1 treated with various concentrations of imatinib (*A*), chloroquine (*B*), or designated combinations of imatinib and chloroquine (*C*). The combination index as determined by Chou–Talalay analysis is shown in *D*. Synergy, additivity, and antagonism are defined as CI < 1, CI = 1, and CI > 1, respectively.

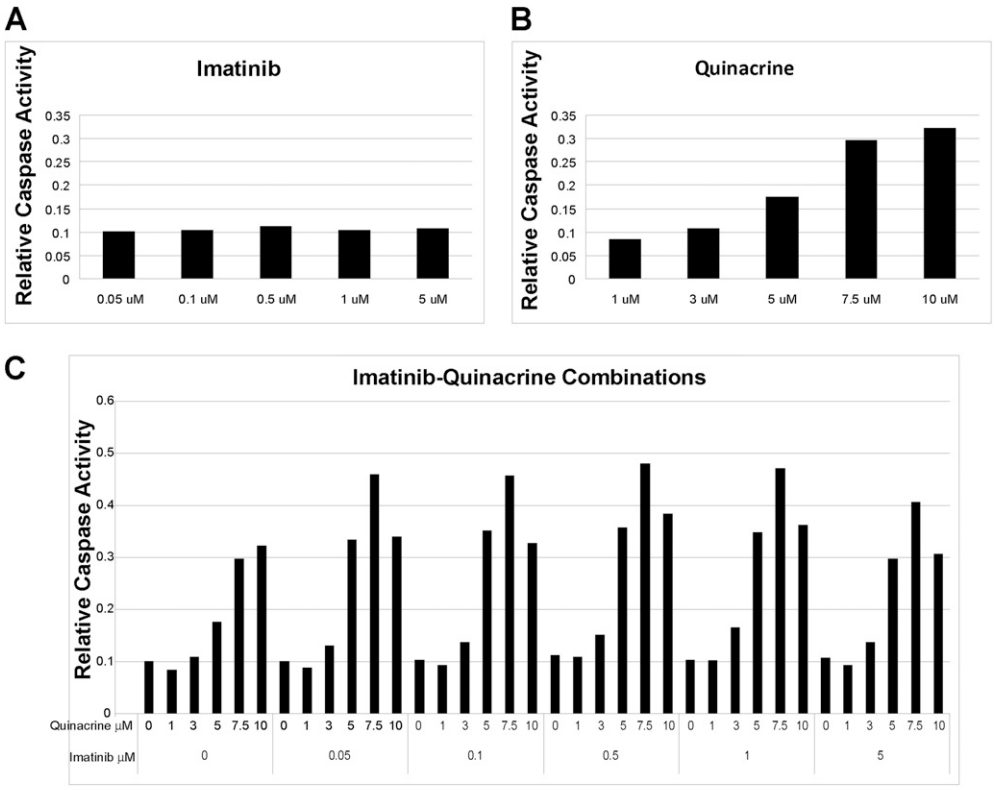

D

Combination Index					
Quinacrine (μM)	Imatinib (μM)				
	0.05	**0.1**	**0.5**	**1**	**5**
1	>1	>1	0.580	>1	>1
3	>1	>1	0.956	0.831	>1
5	0.404	0.364	0.352	0.373	0.507
7.5	0.301	0.305	0.271	0.283	0.400
10	0.778	0.843	0.605	0.688	0.953

Fig. S8. Evaluation of synergistic effect on apoptosis between imatinib and quinacrine by Chou-Talalay analysis. Caspase 3/7 activity of GIST-T1 treated with various concentrations of imatinib (*A*), quinacrine (*B*) or designated combinations of imatinib and quinacrine (*C*). The combination index as determined by Chou-Talalay analysis is shown in *D*. Synergy, additivity, and antagonism are defined as CI < 1, CI = 1, and CI > 1, respectively.

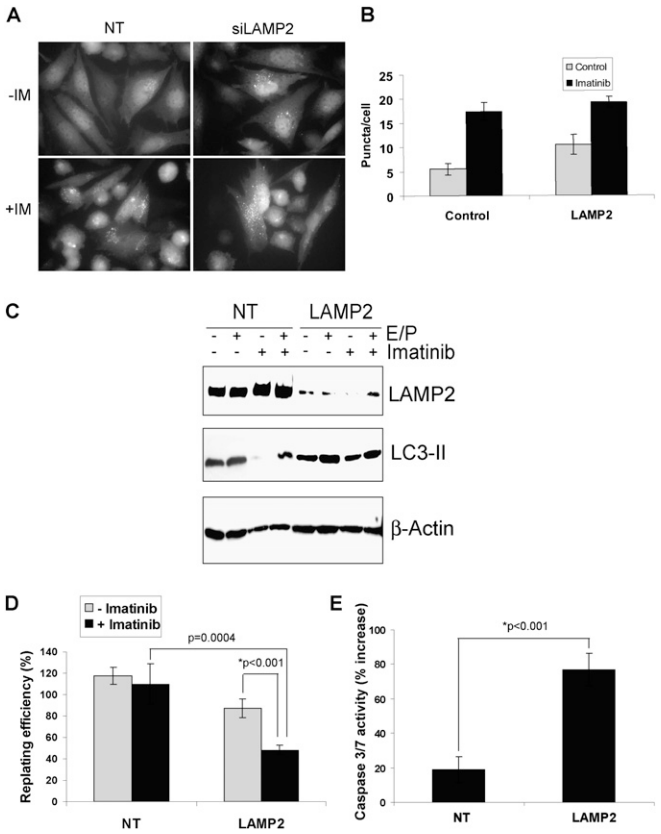

Fig. S9. Inhibition of lysosomal fusion inhibits imatinib-induced autophagy in GIST. (*A*) Representative images of GFP puncta in GIST-T1 cells expressing GFP-LC3 grown in complete media with or without imatinib after transfection with LAMP2 siRNA. (*B*) Quantification of GFP puncta per cell in GIST-T1 cells with or without 1 μM imatinib after transfection with LAMP2 siRNA. (*C*) Autophagy was evaluated in cell lysates with or without 1 μM imatinib after transfection with LAMP2 siRNA. Knockdown was verified by immunoblotting with antibodies to LAMP2, LC3, or β-actin. (*D*) Clonogenic replating efficiency of cells after treatment with or without 1 μM imatinib in LAMP2-depleted cells for 48 h. Replating efficiency was calculated at the number of colonies formed divided by the number of cells originally plated. Results are the mean ± SD from three independent experiments. (*E*) Caspase 3/7 activity was measured in LAMP2-depleted cell lines with or without administration of 1 μM imatinib for 24 h. The data are plotted as percent increase in caspase 3/7 activity relative to untreated controls. NT, nontargeting siRNA pool. *P* values indicated with an asterisk are based on statistical analysis of synergy between imatinib and inhibition of autophagy (see details in *SI Methods*).